



HAL
open science

Ruthenium complexes featuring cooperative phosphine-pyridineiminophosphorane (PNN) ligands: synthesis, reactivity and catalytic activity

Thibault Cheisson, Louis Mazaud, Audrey Auffrant

► To cite this version:

Thibault Cheisson, Louis Mazaud, Audrey Auffrant. Ruthenium complexes featuring cooperative phosphine-pyridineiminophosphorane (PNN) ligands: synthesis, reactivity and catalytic activity. Dalton Transactions, 2018, 47 (41), pp.14521-14530. 10.1039/x0xx00000x . hal-03483415

HAL Id: hal-03483415

<https://hal.science/hal-03483415v1>

Submitted on 16 Dec 2021

HAL is a multi-disciplinary open access archive for the deposit and dissemination of scientific research documents, whether they are published or not. The documents may come from teaching and research institutions in France or abroad, or from public or private research centers.

L'archive ouverte pluridisciplinaire **HAL**, est destinée au dépôt et à la diffusion de documents scientifiques de niveau recherche, publiés ou non, émanant des établissements d'enseignement et de recherche français ou étrangers, des laboratoires publics ou privés.

Ruthenium complexes featuring cooperative phosphine-pyridine-iminophosphorane (PNN) ligands: synthesis, reactivity and catalytic activity.

Received 00th January 20xx,
Accepted 00th January 20xx

DOI: 10.1039/x0xx00000x

www.rsc.org/

Thibault Cheisson, Louis Mazaud, and Audrey Auffrant*

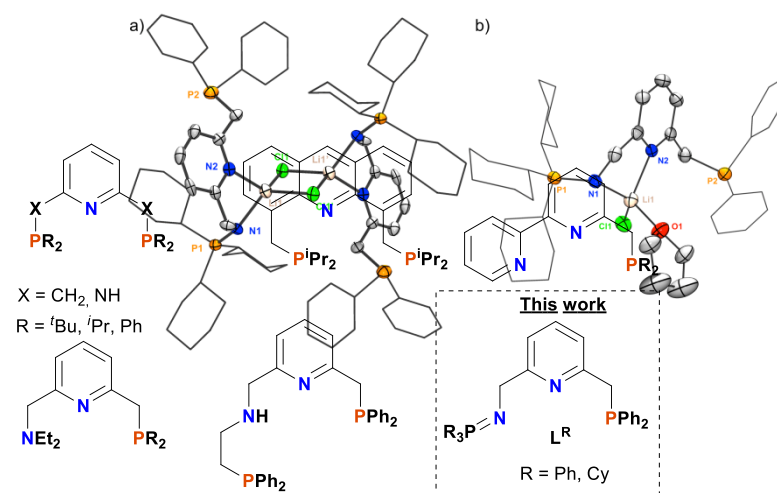
The coordination to ruthenium(II) centres of two phosphine-pyridine-iminophosphorane ligands L^R ($PPh_2CH_2(C_6H_3N)CH_2N=PR_3$, R = Ph or Cy) differing by the nature of the substituent of the P=N phosphorus was explored. Coordination to $[RuCl_2(PPh_3)_3]$ afforded complexes $[RuL^RCl_2(PPh_3)]$ that were successfully deprotonated at the acidic phosphinomethyl position. With L^{Cy} , coordination led to a mixture of two isomers. Complexes $[RuL^R(HCl)(PPh_3)]$ were similarly obtained from $[RuHCl(PPh_3)_3]$. The stability of these complexes depends on the ligand substitution pattern; with L^{Ph} a CH activation process took place, while $[RuL^{Cy}HCl(PPh_3)]$ was thermally stable. Deprotonation of this latter complex was achieved and gave a catalytically competent species for the acceptorless dehydrogenative coupling of alcohols.

Introduction

The development of organometallic complexes incorporating active or cooperative ligands has received considerable attention.¹ In such systems, key elementary bond-breaking and/or -forming steps involve both the ligand and the metal, the latter not varying its oxidation state during the process. Pioneering works of the Noyori group have demonstrated the beneficial effect of the presence of an NH bond in the coordination sphere of ruthenium complexes to achieve fast and efficient transfer hydrogenation of ketones or imines. In the key step of the catalytic cycle, the sp^2 carbon is reduced by a metallic hydride whereas the proton going on the heteroatom (N or O) is shuttled by the coordinated amino group.² Since then, a variety of catalytic systems involving the reversible protonation of a coordinated nitrogen-based moiety has been used for (de)hydrogenation processes.³ The reaction can also be assisted by the secondary coordination sphere, for instance a hydroxyl group.^{3c,4} Few years ago, Milstein and coworkers evidenced another type of cooperativity using lutidine-based pincer systems, in which the reversible deprotonation of the phosphinomethyl group lead to a formally dearomatized pyridine.^{1d,1g,5} Many variations were proposed on this scaffold; the benzylic CH_2 group was replaced by an oxygen atom⁶ or an amine function,⁷ the acridine skeleton⁸ was also used in place of the pyridine one (Chart 1). One of the coordinating phosphine was also changed for a nitrogen donor such as a pyridine,⁹ a pyridone,¹⁰ or a dialkylamine.¹¹ In the latter case, the hemilability of the amine group remarkably impacted the outcome of catalytic reactions compared to what observed with an analogous PNP ligand.¹¹ This prompted us to synthesise another type of PNN ligand combining a proton responsive phosphinomethyl moiety and an iminophosphorane ($N=PR_3$) group. The latter is a strong σ and π donor,¹² which is capable of hemilability.¹³ We previously reported the coordination of such a ligand (L^{Ph} ,

Chart 1) to palladium centres and evidenced the reactivity of the phosphinomethyl arm.¹⁴ In this paper, we examine the coordination of two iminophosphorane containing PNN pincer ligands (L^{Ph} and L^{Cy} , Chart 1) to ruthenium(II) and the reactivity of their ruthenium-hydride complexes. The catalytic dehydrogenative coupling of alcohols into esters is also reported.

Chart 1: Examples of cooperative PNP, PNNP and PNN ligands



Results and discussion

Ligands synthesis and structure

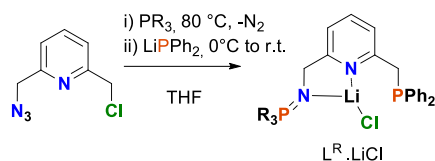
The synthesis of ligand L^{Ph} was previously published¹⁴ and L^{Cy} was prepared in a similar one-pot procedure using 2-(azidomethyl)-6-(chloromethyl)pyridine as the key intermediate (Scheme 1). The iminophosphorane function was first introduced by a Staudinger reaction using tricyclohexylphosphine. The greater bulkiness of the cyclohexyl groups increased the kinetic stability of the intermediate phosphazide.¹⁵ Therefore, the mixture was refluxed to complete the extrusion of N_2 , as confirmed by *in-situ* $^{31}P\{^1H\}$ NMR spectroscopy showing a singlet at $\delta_p = 22.3$ ppm

LCM, CNRS-Ecole polytechnique, Université Paris-Saclay, F-91128 Palaiseau Cedex
audrey.auffrant@polytechnique.edu

* Footnotes relating to the title and/or authors should appear here.

Electronic Supplementary Information (ESI) available: [details of X-ray data and $^{31}P\{^1H\}$ NMR spectra of all complexes as well as 1H NMR spectra of 1^{Ph} , 2^{Ph} , and 4].
See DOI: 10.1039/x0xx00000x

corresponding to the iminophosphorane. Then, a freshly prepared solution of lithium diphenylphosphide in THF was slowly added at 0 °C. After 1 h stirring, the formation of the phosphine-iminophosphorane derivative was evidenced by $^{31}\text{P}\{^1\text{H}\}$ NMR spectroscopy; two broad signals were observed at 30.4 and -10 ppm corresponding respectively to the iminophosphorane and the phosphine groups.



Scheme 1: Synthesis of ligand $\text{L}^{\text{R}}.\text{LiCl}$

The ligand L^{Cv} was isolated in 90% yield as a lithium chloride adduct. Two signals corresponding to the benzylic protons were observed in the ^1H NMR spectrum (THF- d_8): a doublet at 4.62 ppm corresponding to those on the iminophosphorane arm ($^3J_{\text{P,H}} = 15.0$ Hz) and one broad singlet at 3.94 ppm for those on the phosphine arm as determined with 2D ^1H - ^{31}P correlation. The absence of significant $^2J_{\text{P,H}}$ is typical of this scaffold and was previously documented.^{14,16} Single crystals were obtained by evaporation of a chloroform solution from which $\text{L}^{\text{Cv}}.\text{LiCl}$ crystallized as a dimer (Figure 1a) with bridging chlorides. The lithium cation exhibits a distorted tetrahedral geometry ($\tau^4 = 0.87$)¹⁷ due to the bidentate coordination of L^{Cv} , through the pyridine and iminophosphorane moieties. On the contrary, the phosphine arm is free without any supplementary interaction in the crystal packing. The P=N bond length was measured at 1.579(4) Å, which is comparable to the bonds measured in the corresponding bis(iminophosphorane) derivative (1.574(2) and 1.567(2) Å)^{13a} suggesting only a limited interaction with the lithium cation. When recrystallized in presence of THF, a solvated monomer was observed (Figure 1b). In that structure also, only the iminophosphorane and the pyridine are coordinated to the lithium cation, the phosphine remaining free. The deformation of the tetrahedron around the lithium ($\tau^4 = 0.86$)¹⁷ is similar to that observed in the dimeric structure as a result of L^{Cv}

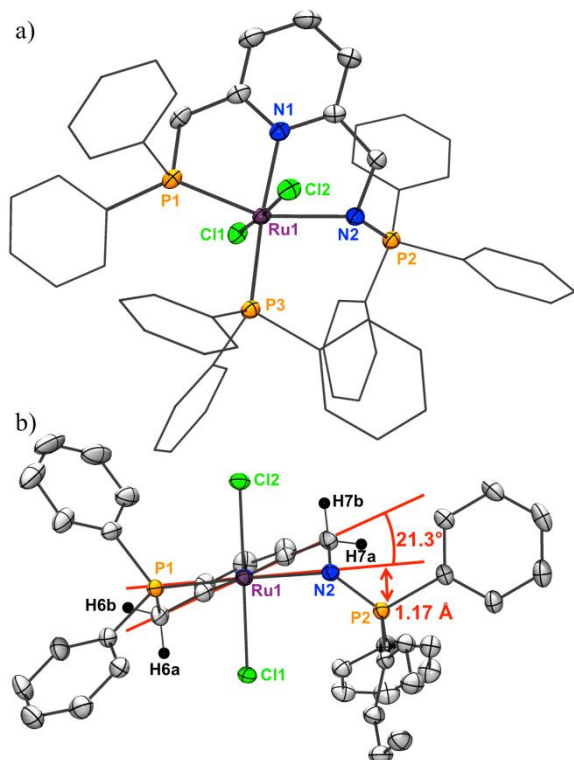
geometry (N1–Li1–N2 = 84.1(3)° in $\text{L}^{\text{Cv}}.\text{LiCl}(\text{THF})$ and 81.6(4) in $[\text{L}^{\text{Cv}}.\text{LiCl}]_2$). There is not much change in the iminophosphorane bond length measured at 1.582(3) Å.

Figure 1. Thermal ellipsoids plots of $[\text{L}^{\text{Cv}}.\text{LiCl}]_2$ (a) and $\text{L}^{\text{Cv}}.\text{LiCl}(\text{THF})$ (b); hydrogen atoms were omitted, cyclohexyl and phenyl groups were depicted in a wire-frame model for clarity. Only one of the two independent molecules of $\text{L}^{\text{Cv}}.\text{LiCl}(\text{THF})$ present in the asymmetric unit is presented. Selected bond lengths (Å) and angles (°): $[\text{L}^{\text{Cv}}.\text{LiCl}]_2$: N1–P1 1.579(4), N1–Li1 2.05(1), N2–Li1 2.17(1), Li1–Cl1 2.31(1), Li1–Cl1' 2.38(1); P1–N1–Li1 130.5(4), N1–Li1–N2 81.6(4), N1–Li1–Cl1 126.8(5), N1–Li1–Cl1' 114.0(5), N2–Li1–Cl1 123.0(5), N2–Li1–Cl1' 108.8(4), Li1–Cl1–Li1' 78.1(4), Cl1–Li1–Cl1' 101.9(4). $\text{L}^{\text{Cv}}.\text{LiCl}(\text{THF})$: N1–P1 1.583(3), N1–Li1 2.014(6), N2–Li1 2.2114(7), Li1–Cl1 2.284(6), Li1–O1 2.002(6); P1–N1–Li1 129.1(2), N1–Li1–Cl1 129.2(3), N2–Li1–Cl1 119.6(3), N1–Li1–N2 84.1(2), O1–Li1–Cl1 110.2(3), O1–Li2–N1 102.4(3).

Synthesis and deprotonation of ruthenium dichloride complexes

Coordination of L^{Ph} and L^{Cv} with various Ru^{II} precursors was next attempted with mixed results.[‡] Reaction between $\text{L}^{\text{Ph}}.\text{LiCl}$ and $[\text{RuCl}_2(\text{PPh}_3)_3]$ was rapid at room temperature. After 1 h in-situ $^{31}\text{P}\{^1\text{H}\}$ NMR spectroscopy showed the appearance of four signals: two doublets at 39.1 ($^2J_{\text{P,P}} = 34.0$ Hz) and 44.7 ppm ($^3J_{\text{P,P}} = 19.5$ Hz) and a doublet of doublets at 54.3 ppm ($J_{\text{P,P}} = 34.0$ and 19.5 Hz) corresponding to $[\text{RuL}^{\text{Ph}}\text{Cl}_2(\text{PPh}_3)]$ ($\mathbf{1}^{\text{Ph}}$) (Figure S1) as well as one singlet at -5 ppm characteristic of free triphenylphosphine. The reaction mixture was filtered and the filtrate was evaporated. The triphenylphosphine was removed by washing with light petroleum ether to deliver complex $[\text{RuL}^{\text{Ph}}\text{Cl}_2(\text{PPh}_3)]$ in 88% yield. The ^1H NMR spectrum of $\mathbf{1}^{\text{Ph}}$ at room temperature was poorly defined with broadened resonances. At -60 °C, in CDCl_3 , two AMX systems were observed showing that the benzylic protons located on the iminophosphorane and phosphine arms are diastereotopic (Figure S2). At this temperature, the complex has no planar symmetry in solution (C_1), which can be explained by: (i) an apical position of the PPh_3 ancillary ligand, or (ii) a loss of planar symmetry due to the coordination of the triphenylphosphine in the equatorial plane. The latter hypothesis was confirmed by X-ray diffraction studies on single crystals obtained by diffusion of *n*-pentane into a concentrated benzene solution (Figure 2a).

The ruthenium atom is at the centre of a distorted octahedron imposed by the meridional coordination of the pincer ligand. The N2–Ru1–N1 and P1–Ru1–N1 angles were measured at 75.6(1) ° and 80.98(7) ° respectively. The chlorine atoms occupy the apical positions and the triphenylphosphine is coordinated *trans* to the pyridine. This structure can be compared to a reported ruthenium(II) complex featuring a tetradentate PNNP ligand, in which the supplementary phosphine moiety is directly linked to the amine function (Figure 1).¹⁸ The bond lengths and angles measured around the ruthenium atom were similar to those reported in this structure. However, the distortion from planarity is larger in **1^{Ph}**, the pyridine ring is deviated by 21.3° from the main



coordination plane (P1–N1–N2–P3) to compare with 3.6° in the [RuCl₂(PNNP)] precedent, and P2 is distant by 1.17 Å from this plane (Figure 2b). These deformations explain well the marked magnetic non-equivalence observed by ¹H NMR spectroscopy at -60 °C for the benzylic protons H_{6a/6b} and H_{7a/7b} (see Figure S2). The interconversion between the two conformations is believed to be hindered by the coordinated PPh₃ ligand and explains the low resolution of the proton NMR spectrum at room temperature. Comparable fluxional behaviours were often observed in the subsequent complexes.

Figure 2. Thermal ellipsoid plots of [RuL^{Ph}Cl₂(PPh₃)] (**1^{Ph}**): (a) perspective; (b) In the P3N1 direction (with PPh₃ ligand omitted). Unless depicted, hydrogen atoms were omitted; some phenyl groups were depicted in a wire-frame model for clarity. Selected bond lengths (Å) and angles (°): N2–P2 1.600(2), N2–Ru1 2.249(2), P1–Ru1 2.2537(7), N1–Ru1 2.103(2), P3–Ru1 2.3545(7), Cl1–Ru1 2.4168(7), Cl2–Ru1 2.4169(7); N2–Ru1–P1 156.42(6), N1–Ru1–P3 171.64(7), Cl1–Ru1–Cl2 175.74(3), N2–Ru1–N1 75.6(1), P1–Ru1–N1 80.98(7), P3–Ru1–N2 100.78(6), P3–Ru1–P1 102.80(3), N1–Ru1–Cl1 88.47(7), N2–Ru1–Cl1 91.10(6), P1–Ru1–Cl1 85.20(3), P3–Ru1–Cl1 99.22(3), N1–Ru1–Cl2 87.29(7), N2–Ru1–Cl2 88.19(6), P1–Ru1–Cl2 93.78(3), P3–Ru1–Cl2 85.03(3).

Similarly, **L^{Cy}** was coordinated to [RuCl₂(PPh₃)₃]. After extraction in dichloromethane, two sets of signals were observed in the ³¹P{¹H} NMR spectrum (Figure S3) indicating the presence of two isomers differing by the relative position of the ancillary PPh₃. After workup, the mixture of isomers

[RuL^{Cy}Cl₂(PPh₃)] (**1^{Cy}**) was obtained in 65 % yield. Single crystals of the *cis*-chloride isomer were obtained by diffusion of light petroleum ether to dichloromethane solutions (Figure 3). The different chemical environment of the chlorine atoms is evidenced by a difference in Ru–Cl bond lengths, Ru1–Cl2 is longer than Ru1–Cl1 (2.4730(1) vs 2.4354(8) Å) because of the stronger *trans* influence of PPh₃. As for **1^{Ph}**, there is a strong deformation compare to an ideal octahedron as the angles N1–Ru1–N2 and P2–Ru1–N2 were measured at 77.9(1) and 82.65(7)° respectively. Moreover, the apical position of the triphenylphosphine tilts the N1–P1 bond away from the mean coordination plane, P1 being located at 0.94 Å. Finally, the *trans* isomer can be selectively extracted in toluene-*d*₈ (Figure S4) and characterized by ¹H NMR spectroscopy at -40°C demonstrating a C₁ symmetric complex as observed for **1^{Ph}**.

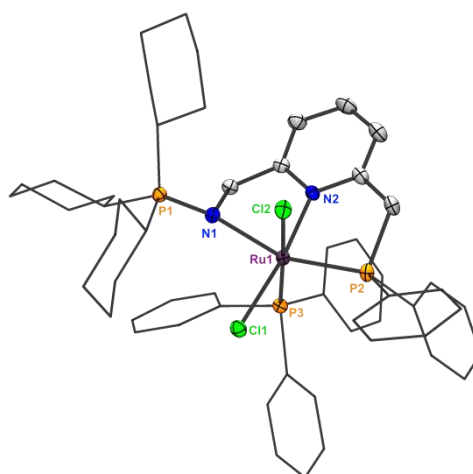
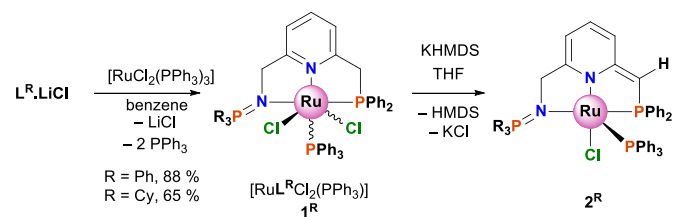


Figure 3: Thermal ellipsoid plots of [RuL^{Cy}Cl₂(PPh₃)] (**1^{Cy}**). Hydrogen atoms were omitted; cyclohexyl and phenyl groups were depicted in a wire-frame model for clarity. Selected bond lengths (Å) and angles (°): N1–P1 1.609(3), N1–Ru1 2.245(3), P2–Ru1 2.2603(8), N2–Ru1 2.045(2), P3–Ru1 2.2817(8), Cl1–Ru1 2.4354(8), Cl2–Ru1 2.4730(1); N1–Ru1–P2 159.61(7), N2–Ru1–Cl1 171.88(7), P3–Ru1–Cl2 174.58(3), N1–Ru1–N2 77.9(1), P2–Ru1–N2 82.65(7), Cl1–Ru1–N1 96.42(7), Cl1–Ru1–P2 83.17(3), N2–Ru1–P3 99.06(8), N1–Ru1–P3 91.93(7), P2–Ru1–P3 97.25(3), Cl1–Ru1–P3 86.87(3), N1–Ru1–Cl2 89.40(6), N2–Ru1–Cl2 86.36(7), P2–Ru1–Cl2 83.17(3), Cl1–Ru1–Cl2 87.76(3).

We previously demonstrated that palladium complexes of **L^{Ph}** were susceptible of benzylic deprotonation α to the phosphine fragment.¹⁴ Hence, deprotonations of **1^{Ph}** and **1^{Cy}** were investigated with potassium hexamethyldisilazane (KHMDs, Scheme 2).



Scheme 2: Coordination of **L^{Ph}** and **L^{Cy}** to [RuCl₂(PPh₃)₃] and benzylic deprotonation

In all cases, the solutions turned from orange to red. The ³¹P{¹H} NMR spectrum of [RuL^{Ph}*Cl(PPh₃)]⁺ (**2^{Ph}**) in C₆D₆ (Figure S4) showed three signals: a doublet at 34.9 ppm (³J_{P,P} = 19.5 Hz), a doublet of doublets at 51.8 (³J_{P,P} = 19.5 and ²J_{P,P} = 56.5) and a doublet at 83.5 ppm (²J_{P,P} = 56.5 Hz), which were assigned respectively to the iminophosphorane, the diphenylphosphino group and the triphenylphosphine ligand. The deprotonation induces only small changes in the

chemical shifts of these first two P nuclei whereas PPh_3 is largely deshielded ($\Delta\delta_p \sim 40$ ppm), this chemical shift and the magnitude of $^2J_{p,p}$ are comparable to what observed in *cis*- $\mathbf{1}^{\text{Cy}}$ suggesting an apical position of this ligand relative to the pincer moiety. The ^1H NMR spectrum evidenced the partial loss of aromaticity in the pyridine ring with signals at 6.35, 6.09, and 5.23 ppm. The benzylic proton of the phosphine arm was observed at 3.70 ppm as a doublet ($^2J_{p,h} = 3.5$ Hz), integrating for one proton confirming the locus of the deprotonation. Interestingly, the benzylic protons on the iminophosphorane arm gave an ABX pattern integrating for 2 protons between 3.85 and 4.05 ppm. Resolution of this signal (Figure S6) indicated very different $^3J_{p,h}$ constants (41.0 and -6.0 Hz) for the two diastereotopic protons. This large magnetic non-equivalence further suggested a large tilting of the iminophosphorane moiety out of the mean coordination plane, confirming the apical location of the PPh_3 ligand. This complex was not stable in solution for an extended period precluding the recording of its ^{13}C NMR spectrum.

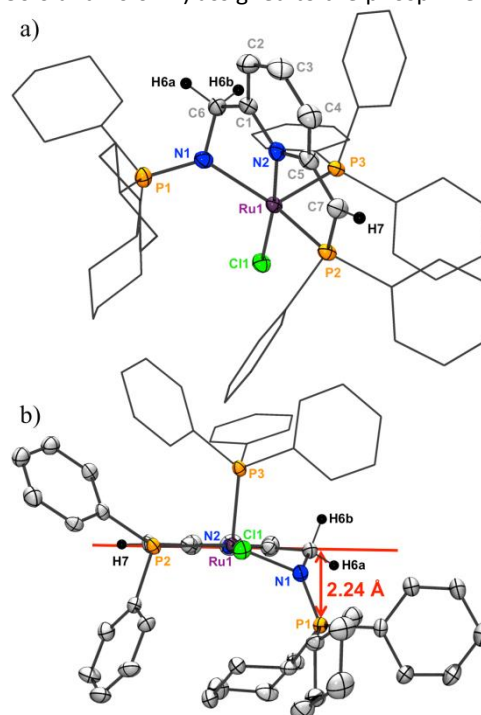
The $^{31}\text{P}\{^1\text{H}\}$ and ^1H NMR spectra of $\mathbf{2}^{\text{Cy}}$ are very similar to those of $\mathbf{2}^{\text{Ph}}$. The phosphorus nuclei resonated as a doublet at 79.2 ppm ($^2J_{p,p} = 52.0$ Hz) for the PPh_3 group, a doublet of doublet at 47.0 ppm ($J_{p,p} = 52.0$ and 21.5 Hz) for the CHPPH_2 moiety and a doublet at 53.9 ppm ($^3J_{p,p} = 21.5$ Hz) for the iminophosphorane (Figure S7). The deshielding of the P^{V} atom is due to the modification of substituents. As previously, ^1H NMR spectroscopy evidenced the dearomatization of the pyridine with signals between 5.4 and 6.5 ppm. The benzylic protons appeared as two doublets of doublet at 4.20 and 3.78 ppm whereas the vinylic proton on the phosphine arm resonated at 4.35 ppm as a doublet. The similarity of the NMR data supports an analogous structure for $\mathbf{2}^{\text{Ph}}$ and $\mathbf{2}^{\text{Cy}}$. For the latter, single crystals were obtained allowing an X-ray crystallographic analysis (Figure 4a).

The Ru atom lies in a strongly distorted square pyramidal geometry ($\tau_5 = 0.4$)¹⁹ with the pincer ligand and the chloride anion in the equatorial plane and the triphenylphosphine *trans* to a vacant site in the apical position, as anticipated from NMR data. The distances to ruthenium do not change much upon deprotonation. The benzylic deprotonation is confirmed by the localization of only one proton on C7 and the loss of aromaticity of the pyridine ring as evidenced by the alternation of long and short bonds. This also induces a shortening of the P2-C7 and C7-C5 measured at 1.747(4) and 1.383(6) Å respectively compared to 1.855(3) and 1.504(4) Å in $\mathbf{1}^{\text{Cy}}$. The distortion to the square pyramid geometry is mostly generated by the iminophosphorane moiety. The $\text{N}=\text{PCy}_3$ fragment is located in the hemisphere opposite to the PPh_3 , with N1 and P1 respectively at 0.76 and 2.24 Å from the mean Ru1-Cl1-N2-P2 plane. Contrary to $\mathbf{1}^{\text{R}}$, the mean coordination plane is now nearly coplanar with the dearomatized pyridine ring plane (Figure 4b).

Synthesis and reactivity of ruthenium hydride complexes

In order to develop cooperative catalysts from those ruthenium complexes, the introduction of a metallic hydride was attempted. Reaction of NaBH_4 or KBET_3H with $\mathbf{1}^{\text{Ph}}$ or $\mathbf{1}^{\text{Cy}}$

gave intractable mixtures of compounds. Similarly, reaction of $\mathbf{1}^{\text{R}}$ (in presence of a base) or $\mathbf{2}^{\text{R}}$ ($\text{R} = \text{Ph}, \text{Cy}$) under H_2 failed. We therefore turned our attention to a ruthenium precursor containing a hydride. We first used $[\text{RuHCl}(\text{CO})(\text{PPh}_3)_3]$ but the coordination is accompanied by the formation of phosphine oxide due to the aza-Wittig reaction between the coordinated $\text{N}=\text{P}$ moiety and CO .²⁰ $[\text{RuHCl}(\text{PPh}_3)_3]$ was then employed. Its reaction with \mathbf{L}^{Ph} in toluene or benzene was rapid leading to a new compound $[\text{RuL}^{\text{Ph}}\text{HCl}(\text{PPh}_3)]$ ($\mathbf{3}^{\text{Ph}}$, Scheme 3) characterized in $^{31}\text{P}\{^1\text{H}\}$ NMR by a doublet of doublet centred at 72.0 ppm ($^2J_{p,h} = 36.0$ and 16.0 Hz) assigned to the phosphine group, and

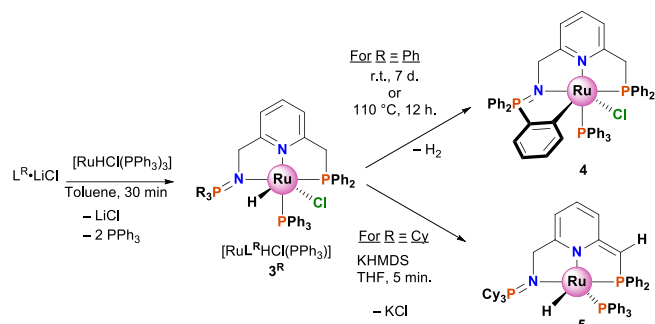


two doublets at 59.7 and 41.1 ppm corresponding respectively to PPh_3 and the iminophosphorane (Figure S8).

Figure 4: Thermal ellipsoid plots of $[\text{RuL}^{\text{Cy}}\text{Cl}_2(\text{PPh}_3)]$ ($\mathbf{2}^{\text{Cy}}$): (a) perspective; (b) in the Ru1N2 direction H6a, H6b and, H7 were located on the density map and isotropically refined. Hydrogen atoms, unless depicted, were omitted; some cyclohexyl and phenyl groups are depicted in a wire-frame model for clarity. Selected bond lengths (Å) and angles ($^\circ$): N1-P1 1.614(4), N1-Ru1 2.181(3), P2-Ru1 2.260(1), N2-Ru1 2.034(3), P3-Ru1 2.200(1), Cl1-Ru1 2.421(1), N2-C1 1.360(5), C1-C2 1.361(6), C2-C3 1.407(7), C3-C4 1.357(7), C4-C5 1.424(6), C5-N2 1.392(5), C5-C7 1.383(6), P2-C7 1.747(4), C7-H7 0.92(5); N1-Ru1-P2 149.9(1), N2-Ru1-Cl1 174.3(1), N1-Ru1-N2 78.6(1), P2-Ru1-N2 81.6(1), Cl1-Ru1-N1 96.1(1), Cl1-Ru1-P2 102.32(4), N2-Ru1-P3 94.6(1), N1-Ru1-P3 94.6(1), P2-Ru1-P3 96.47(4), Cl1-Ru1-P3 89.04(4).

The ^1H NMR spectrum showed a characteristic doublet of doublet at -16.6 ppm ($^2J_{p,h} = 31.5$ and 22.5 ppm) in C_6D_6 . The magnitude of these $J_{p,h}$ coupling constants and their similarity indicated an hydride *cis* to the two phosphine groups and a triphenylphosphine therefore in apical position.

Complex $\mathbf{3}^{\text{Ph}}$ is not stable and evolved slowly in solution to a new product. The reaction was finished within a week at room temperature or overnight in refluxing toluene. The obtained complex $\mathbf{4}$ was characterized by three $^{31}\text{P}\{^1\text{H}\}$ NMR signals: two doublets at 53.3 and 48.4 ppm ($^2J_{p,p} = 31.0$ Hz) and a singlet at 48.2 ppm (Figure S9). The latter was assigned to the iminophosphorane group thanks to $^{31}\text{P}-^1\text{H}$ and $^{13}\text{C}-^1\text{H}$ correlation spectra.



Scheme 3: Reaction of L^R with $[RuHCl(PPh_3)_3]$ and further reactivity

The 1H NMR spectrum lacks any hydride resonance and is very complicated, revealing a largely dissymmetric structure. When the reaction was conducted in a sealed tube, the formation of H_2 was evidenced by a signal at 4.50 ppm in the 1H NMR spectrum. Fortunately, single crystals were obtained allowing understanding the structure of **4** by X-ray diffraction analysis (Figure 5).

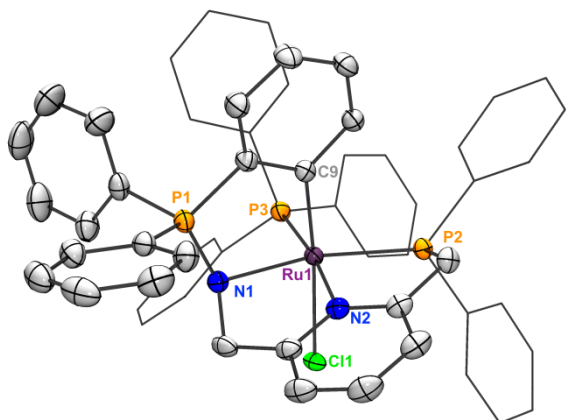


Figure 5: Thermal ellipsoid plot of **4**. Hydrogen atoms and 1.5 benzene molecules were omitted; some phenyl groups are depicted in a wire-frame model for clarity. Selected bond lengths (Å) and angles (°): N1–P1 1.612(2), N1–Ru1 2.193(2), P2–Ru1 2.2821(8), N2–Ru1 2.094(2), P3–Ru1 2.3087(8), Cl1–Ru1 2.5412(7), C9–Ru1 2.072(3); N1–Ru1–P2 157.49(7), N2–Ru1–P4 173.08(7), C9–Ru1–Cl1 172.69(8), N1–Ru1–N2 76.6(1), P2–Ru1–N2 80.94(7), P2–Ru1–P3 104.23(3), N1–Ru1–P3 98.26(7), Cl1–Ru1–N1 88.08(7), Cl1–Ru1–P2 91.65(3), Cl1–Ru1–N2 86.35(7), Cl1–Ru1–P3 88.88(3), C9–Ru1–N2 88.9(1), C9–Ru1–N1 85.4(1), C9–Ru1–P3 95.34(8), C9–Ru1–P2 80.94(7).

The solid-state structure of **4** shows a cyclometalated complex resulting from CH activation at an iminophosphorane phenyl substituent and concomitant loss of H_2 .²¹ The ruthenium centre adopts a distorted octahedral geometry, with N2–Ru–P3 and N1–Ru–P2 angles at 172.8(1) and 157.25(8)°. Noteworthy P2, P3, N1, N2 and Ru1 are almost coplanar, the maximum distance to the mean coordination plane being 0.175 Å. However, because of the cyclometalation, the iminophosphorane is markedly distorted; Ru1–N1–P1 is measured at 111.4(1)° and P1 is 1.47 Å from the mean coordination plane, which is almost perpendicular to the plane defined by the N1, P1, C9, and Cl1 atoms, the angle measures 89.4°. Such a distortion is proposed to limit the magnetic coupling between P1 and P2 and therefore cancelling out the $^3J_{P,P}$ coupling, as observed experimentally (Figure S9). The

newly formed C9–Ru1 bond, measured at 2.072(3) Å, is *trans* to the chloride anion, which therefore experiences a large *trans* influence and is further pushed away from the metal than in **1^{Ph}** (Cl1–Ru1 at 2.5412(7) vs 2.4168(7) Å).

Resulting from the lack of any symmetry, the 1H and ^{13}C NMR spectra of **4** were difficult to fully assign. However, extensive 1H , ^{31}P , and ^{13}C correlation NMR experiments allowed the characterization of the key features: (i) the protons α to the phosphine are diastereotopic and appear as an AMX system with two doublets of doublets at 3.69 ($^2J_{H7a,H7b} = 15.5$ Hz, $^2J_{P,H7} = 8.0$ Hz) and 4.18 ppm ($^2J_{H7a,H7b} = 15.5$ Hz, $^2J_{P,H7b} = 11.5$ Hz). (ii) Those of the iminophosphorane arm also give an AMX system with a broad pseudo triplet at 4.00 ppm ($^2J_{H6a,H6b} = 17.5$ Hz, $^3J_{P1,H6} = 16.0$ Hz), whereas the other resonance was localized at 6.69 ppm ($^2J_{H6a,H6b} = 17.5$ Hz, $J_{P1,H6b} \sim 39$ Hz) (Figure S10) This unusual chemical shift for benzylic protons, as well as the large non-equivalence in the $^3J_{P,H}$ coupling constants are reminiscent of those observed in **2^R** and seem characteristic of ‘out of the plane’ deformation of the N=P bond. (iii) All protons of the cyclometalated ring are shielded, the chemical shifts varying between 6.35 and 7.40 ppm. (iv) The ^{13}C NMR spectrum of the cyclometalated ring were assigned, in particular the metallated carbon C9 was observed at 191.2 ppm in the $^{13}C\{^{31}P\}$ spectrum. This value is in good agreement with those reported by Urriolabeitia’s group for cyclometalated ruthenium-iminophosphorane complexes.²² Cyclometallation reactions at the acidic protons of an iminophosphorane P-substituents were previously documented.²³ **4** appeared inert when placed under H_2 in THF for 1 day or when reacted with hydride sources (catecholborane, pinacolborane or triphenylsilane) at 50 °C for 48 h.

Reasoning that CH activation would be more difficult at the sp^3 carbons of L^{Cy} , we attempted its coordination with $[RuHCl(PPh_3)_3]$. A mixture of isomers (in approximate 1:2 ratio) is formed after one night at room temperature as evidenced by $^{31}P\{^1H\}$ NMR spectroscopy of the crude reaction mixture (Figure S11). The major isomer exhibits three ^{31}P resonances in THF- d_8 ; a broad apparent doublet at 68.0 ($^2J_{P,P} = 37.0$ Hz) a doublet at 65.2 ($^2J_{P,P} = 37.0$ Hz) and a doublet at 51.8 ($^3J_{P,P} \sim 7.5$ Hz) assigned respectively to the PPh₂, PPh₃ and P=N groups thanks to 2D experiments. In $^1H\{^{31}P\}$ NMR spectrum, the benzylic protons of the phosphinomethyl arm were seen as doublets at 3.88 and 4.09 ppm ($^2J_{H,H} = 16.0$ Hz) and those of the iminophosphorane side gave two doublets at 4.85 and 4.75 ppm ($^2J_{H,H} = 15.0$ Hz). The hydride of this major complex resonates at -14.6 ppm. The minor isomer shows in $^{31}P\{^1H\}$ NMR spectroscopy a doublet of doublet at 77.9 ppm ($J_{P,P} \sim 34$ and 16 Hz), a doublet at 58.2 ppm ($J_{P,P} \sim 36$ Hz) and a doublet at 54.4 ($J_{P,P} \sim 16$ Hz). For this complex, the benzylic protons resonate at 5.41 and 3.63 for those on the phosphinomethyl arm and at 4.75 and 4.85 ppm for those close to the iminophosphorane. The hydride of this minor complex was observed at -15.6 ppm (Figure S13).

Crystals of one of the isomer were obtained from a concentrated toluene solution and analysed by X-ray diffraction (Figure 6). This complex presents a distorted octahedral geometry around the Ru centre with the hydride and chlorine atoms in apical positions *trans* to each other. The

triphenylphosphine is trans to the pyridine ligand at 2.276(1) Å from the metal, a much shorter bond compare to that measured in [RuL^{Cy}Cl₂(PPh₃)] in which it faces a chloride. The Ru1-Cl1 bond is longer (2.603(2) Å) than those of the **1^{Cy}** because of the stronger *trans* influence of the hydride. It is also slightly longer than the Ru-Cl bond length measured in the phosphine-pyridine-amine [RuHCl(PNN)(CO)] complex (2.5831(13) Å) in which the chloride is also trans to the hydride.²⁴ As observed in other solution- and solid-state structures of this family of compounds, the phosphorus atom of the iminophosphorane function namely, P2, is pushed away from the mean coordination plane N1–N2–P2–P3 (1.41 Å).

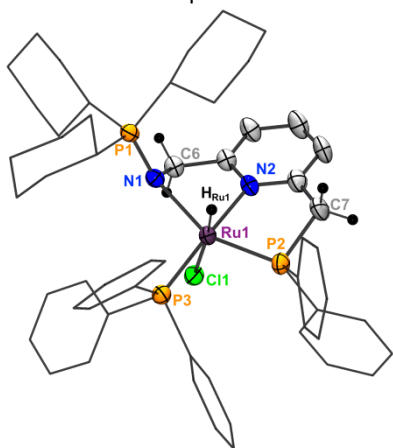


Figure 6. Thermal ellipsoids plot of [RuL^{Cy}HCl(PPh₃)] (**3^{Cy}**); H_{Ru1} was located on the density map and refined isotropically. Hydrogen atoms, unless depicted were omitted, cyclohexyl and phenyl groups are depicted in a wire-frame model for clarity. Only one of the two independent molecules **3^{Cy}** occurring in the asymmetric unit is presented. Selected bond lengths (Å) and angles (°): N1–P1 1.612(3), H_{Ru1}–Ru1 1.57(5), N1–Ru1 2.269(3), P2–Ru1 2.217(1), N2–Ru1 2.107(4), P3–Ru1 2.276(1), Cl1–Ru1 2.603(1); N1–Ru1–P2 154.61(9), H_{Ru1}–Ru1–Cl1 175(2), P3–Ru1–N2 176.3(1), N1–Ru1–N2 75.3(1), P2–Ru1–N2 82.0(1), Cl1–Ru1–N1 87.32(9), Cl1–Ru1–P2 102.51(4), N2–Ru1–Cl1 86.3(1), N1–Ru1–P3 105.70(9), P2–Ru1–P3 97.70(4), Cl1–Ru1–P3 90.18(4), N1–Ru1–H_{Ru1} 89(2), N2–Ru1–H_{Ru1} 96(2), P2–Ru1–H_{Ru1} 82(2), P3–Ru1–H_{Ru1} 87(2).

Besides the presence of two isomers, solutions of **3^{Cy}** have good thermal stability and were stable for days with no apparent sign of degradation validating our hypothesis. With a stable ruthenium hydride complex in hand, we next attempted its benzylic deprotonation. Addition of one equivalent of KHMDS to a THF solution of **3^{Cy}** led to the formation of the dearomatized complex **5** (Scheme 3). Notably the mixture of **3^{Cy}** isomers gave a sole product (in THF-*d*₈) which is characterized by three ³¹P{¹H} resonances (figure S12): two doublets at 99.8 (²J_{P,P} = 60.0 Hz), and 51.5 (³J_{P,P} = 15.0 Hz), and a doublet of doublet at 64.0 ppm (*J*_{P,P} = 60.0 and 15.0 Hz corresponding respectively to the triphenylphosphine, the CHPPH₂ and the iminophosphorane groups. The hydride appears at –12.2 ppm as a doublet of doublet (²J_{P,H} = 50.0 and 14.5 Hz). Selective decoupling experiments allowed assigning the largest ²J_{P,H} constant to the coupling with PPh₃, which is therefore *trans* to the hydride (Figure S13). Complex **5** showed limited stability for a prolonged time in solution. Reasoning that *in situ* generation and the presence of a substrate may increase its lifetime, we investigated its catalytic behaviour for the dehydrogenative coupling of alcohols to esters. Alcohols (neat or in toluene) were refluxed in presence of 0.1 mol % of [RuL^{Cy}HCl(PPh₃)] and 0.2 mol % of KHMDS for 24 h. The

conversion was determined by ¹H NMR analysis of the crude mixture. Results are summarized in Table 1. This acceptorless dehydrogenative coupling was quite efficient with aliphatic alcohols however low conversion was observed with 4-chlorobenzyl alcohol. Nevertheless, this iminophosphorane based catalyst is not as efficient as other ruthenium catalyst featuring an amine based PNN ligand.²⁴⁻²⁵ This may be due to the crowding of the metal coordination sphere because of the presence of the triphenylphosphine.

Table 1: Catalytic acceptorless dehydrogenation of alcohols.

Substrate	T (°C)	Conversion (%) ^a
1-pentanol	138	82
1-hexanol	157	71

$2 \text{ R-CH}_2\text{OH} \xrightarrow[24\text{h, reflux}]{0.1 \text{ mol. \% } \mathbf{3}^{\text{Cy}}, 0.2 \text{ mol. \% KHMDS}} \text{R-CO-CH}_2\text{R} + \text{H}_2$		
benzyl alcohol	115	71
benzyl alcohol ^b	115	76
4-chlorobenzyl alcohol ^b	115	26

^a Determined by ¹H NMR spectroscopy; ^b Reaction performed in toluene.

Conclusions

In conclusion, we described the coordination of two lutidine based phosphine-iminophosphorane PNN ligands to ruthenium(II) centres. Coordination to [RuCl₂(PPh₃)₃] afforded complexes [RuL^RCl₂(PPh₃)] (**1^R**). Formation of two isomers was evidenced with **L^{Cy}**. The designed non-innocence of the ligands was confirmed when deprotonations of **1^R** were evidenced at the phosphinomethyl arm to yield [RuL^R*Cl(PPh₃)] (**2^R**). The reaction of **L^R** with [RuHCl(PPh₃)₃] yield [RuL^RHCl(PPh₃)] (**3^R**). The fate of complexes **3^R** was dictated by the nature of the substituent on the phosphorus of the iminophosphorane moiety. **3^{Ph}** underwent a slow CH activation process leading to the cyclometalated complex **4** which proved to be mostly inert. Inversely, **3^{Cy}** was stable and can be cleanly deprotonated at the phosphinomethyl arm to give the catalytically relevant complex [RuL^R*H(PPh₃)] (**5**). The latter complex was able to catalyse the acceptorless dehydrogenation of alcohols to esters with moderate performances. We demonstrated that iminophosphorane-based non-innocent ligands can be catalytically competent with ruthenium centre and learned some design rules to prevent deactivation pathways. Owing to the electronic properties of the iminophosphorane function and its affinity for hard, first row transition metals, such as iron(II) and cobalt(II), we expect such species to be stable and powerful catalysts for similar transformations. Studies in that direction are currently ongoing in our laboratory.

Experimental part

Synthesis

All experiments, unless otherwise stated, were performed under an atmosphere of dry nitrogen or argon using standard

2^{Cy}: [RuL^{Cy}Cl₂(PPh₃)] (**1^{Cy}**) (102 mg, 0.1 mmol) and KH (40 mg, 1 mmol, 10 equiv.) or KHMDS (20 mg, 0.1 mmol, 1 equiv.) were added to a Schlenk flask and stirred in THF (2 mL) for 72 h resulting in a dark red solution which was filtered over a pad of celite. The addition of petroleum ether (10 mL) led to the precipitation of the product. After filtration and washing with Et₂O (3 mL), the product was dried under vacuum to yield [RuL^{Cy}*Cl(PPh₃)] (**2^{Cy}**, 54 mg, 55 %). ³¹P{¹H} NMR (C₆D₆) δ 79.2 (d, ²J_{P,P} = 52.0 Hz, PPh₃), 53.9 (d, ³J_{P,P} = 21.5 Hz, N=P), 47.0 (dd, ²J_{P,P} = 52.0 Hz, ³J_{P,P} = 21.5 Hz, PPh₂). ¹H NMR (C₆D₆) 9.18-9.10 (m, ca. 3H, H_{Ar}), 7.93-7.77 (m, ca. 2H, H_{Ar}), 7.78-7.61 (m, ca. 7H, H_{Ar}), 7.29-7.24 (m, ca. 4H, H_{Ar}), 7.04-6.89 (m, ca. 7H, H_{Ar}), 6.82-6.78 (m, ca. 2H, H_{Ar}), 6.47-6.33 (m, 2H, H₃ and H₄), 5.43 (d, ³J_{H,H} = 6.0 Hz, 1H, H₂), 4.35 (d, ²J_{P,H} = 3.0 Hz, 1H, H₇), 4.19 (AMX, ²J_{H,H} = 15.5 Hz, ³J_{P,H} = 21.5 Hz, 1H, H_{6a}), 3.78 (AMX, ²J_{H,H} = 15.5 Hz, ³J_{P,H} = 19.5 Hz, 1H, H_{6b}), 1.96-0.59 (m, 33H, H_{Cy}).

3^{Ph}: In a glove box, [RuHCl(PPh₃)₃].toluene (25.3 mg, 25 μmol) and L^{Ph}-LiCl (15.3 mg, 25 μmol) were mixed in C₆D₆ (0.75 mL) and stirred for 30 minutes. The solution was transferred to a J-Young NMR tube for spectroscopic analysis. ³¹P{¹H} NMR (C₆D₆) δ 72.0 (dd, ²J_{P,P} = 36.0 Hz, ³J_{P,P} = 16.0 Hz, PPh₂), 59.7 (d, ²J_{P,P} = 36.0 Hz, PPh₃), 41.6 (d, ³J_{P,P} = 16.0 Hz, N=P). ¹H NMR (C₆D₆) δ 8.23-6.73 (m, ca. 41H, H_{Ar}), 6.57 (d, ³J_{H,H} = 5.5 Hz, 1H, H_{Ar}), 5.88 (d, ³J_{H,H} = 5.0 Hz, 1H, H_{Ar}), 5.32 (bs, 1H, H_{6a}), 4.88 (bd, 2H, H₇ and H_{7b}), 3.70-3.61 (m, 1H, H_{6b}), -16.6 (dd, ²J_{P,H} = 31.5 and 22.5 Hz, 1H, RuH).

4: [RuHCl(PPh₃)₃].toluene (71.3 mg, 70 μmol) and L^{Ph}-LiCl (42.7 mg, 70 μmol) were stirred in toluene (5 mL) resulting in a purple solution. The mixture was then refluxed overnight to give a dark red solution. The amount of solvent was reduced to 1.5 mL and petroleum ether (40 mL) was added to enhance the precipitation. The resulting red solid was filtered and washed with petroleum ether (10 mL). After drying under vacuum, **4** was isolated as a red solid (38.6 mg, 57 %). ³¹P{¹H} NMR (C₆D₆) δ 53.3 (d, ²J_{P,P} = 31.0 Hz, PPh₂), 48.4 (d, ²J_{P,P} = 31.0 Hz, PPh₃), 48.2 (s, N=P). ¹H NMR (C₆D₆) δ 7.63-7.54 (m, ca. 6H, H_{Ar}), 7.40 (bd, ³J_{H,H} = 7.5 Hz, H_{10'}), 7.29-6.39 (m, ca. 29H, H_{Ar}, H₃₊₄), 6.70 (not directly observed, localized with HSQC, H₉), 6.69 (dd, ²J_{H,H} = 16.0 Hz, ³J_{P,H} = 38.5 Hz, 1H, H_{6a}), 6.46 (br t, ³J_{H,H} = 7.0 Hz, 1H, H₁₁), 6.35 (t, ³J_{H,H} = 7.5 Hz, 1H, H_{10'}), 6.12 (d, ³J_{H,H} = 7.0 Hz, 1H, H₂), 4.18 (dd, ²J_{H,H} = 15.5 Hz, ³J_{P,H} = 8.0 Hz, 1H, H_{7a}), 4.00 (dd, ²J_{H,H} = 16.0 Hz, ³J_{P,H} = 17.5 Hz, 1H, H_{6b}), 3.69 (dd, ²J_{H,H} = 15.5 Hz, ³J_{P,H} = 11.5 Hz, 1H, H_{7b}). ¹³C NMR (C₆D₆) δ 191.2 (J_{P,C} not observable, C_{9'}), 170.4 (s, C₁), 161.7 (d, ²J_{P,C} = 5.0 Hz, C₅), 145.0 (dd, ³J_{P,C} ~ 13 Hz, ⁴J_{P,C} ~ 6.5 Hz, C_{10'}), 140.2 (d, ¹J_{P,C} = 123.5 Hz, C₈), 133.2 (s, C₃), 132.7 (d, ²J_{P,C} = 9.8 Hz, C₉), 127.2 (d, ⁴J_{P,C} ~ 6 Hz, C₁₁), 118.9 (d, ³J_{P,C} = 13.5 Hz, C₁₀), 118.2 (d, ⁴J_{P,C} = 9.5 Hz, C₄), 116.8 (s, C₂), 59.9 (s, C₆), 47.8 (d, ²J_{P,C} = 26.0 Hz, C₇). 20 others signals in the aromatic region can be detected but not assigned. HRMS (ESI⁺) (C₅₅H₄₆ClN₂P₃Ru): 929.1913 ([M-Cl]⁺; C₅₅H₄₆ClN₂P₃Ru⁺; calcd 929.1933); 464.5967 ([M-Cl]²⁺; C₅₅H₄₆N₂P₃Ru²⁺; calcd 464.5966).

3^{Cy}: [RuHCl(PPh₃)₃].toluene (302.5 mg, 0.3 mmol) and L^{Cy}.LiCl (186.6 mg, 0.3 mmol) were mixed in toluene (5 mL). After overnight stirring, LiCl salt was filtered off, the solution was then concentrated to circa 2 mL and the product was precipitated by addition of pentane (10 mL). The brown precipitate was filtered and washed with pentane (10 mL) and

dried under vacuum to yield [RuL^{Cy}HCl(PPh₃)] (**3^{Cy}**, 241 mg, 82%) as a mixture of two isomers labelled A for the major and B for the minor (A: B ~ 2 : 1). ³¹P{¹H} NMR (THF-d₈) δ 77.9 (dd, ²J_{P,P} ~ 37 Hz and ³J_{P,P} ~ 16 Hz, PPh₂(B)), 68.1 (br d, ²J_{P,P} ~ 34 Hz, PPh₂(A)), 65.2 (d, ²J_{P,P} ~ 37 Hz, PPh₃(A)), 58.2 (d, ²J_{P,P} ~ 34 Hz, PPh₃(B)), 54.4 (d, ³J_{P,P} ~ 16 Hz, P=N(B)) 51.8 (d, ³J_{P,P} ~ 7 Hz, P=N(A)). ¹H{³¹P} NMR (THF-d₈): 8.30 (m, 4H, H_{Ar}(B)) 8.05 (m, 4H, H_{Ar}(B)), 6.5-7.7 (m, ca 48 H, H_{Ar}(A) and H_{Ar}(B)), 6.33 (d, ²J_{H,H} = 15.5 Hz, H₇(A)), 5.41 (d, ²J_{H,H} = 14.5 Hz, 1H, H_{6a}(B)), 4.85 (d, ²J_{H,H} = 15.0 Hz, 1H, H_{7a}(B)), 4.75 (d, ²J_{H,H} = 15.0 Hz, 1H, H_{7b}(B)), 4.15 (d, ²J_{H,H} = 15.5 Hz, 1H, H_{7b}(A)), 4.05 (d, ²J_{H,H} = 16.0 Hz, 1H, H_{6a}(A)), 3.84 (d, ²J_{H,H} = 16.0 Hz, 1H, H_{6b}(A)), 3.63 (m, H_{6b}(B)), 1.5-0.21 (m, ca 22H, H_{Cy}). -14.39 (dd, ²J_{P,H} = 30.4 and 22.6 Hz, 1H, RuH(A)), -15.62 (dd, ²J_{P,H} = 34.0 and 20.9 Hz, 1H, RuH(B)).

5: In a glove box, [RuL^{Cy}HCl(PPh₃)] (**3^{Cy}**, 50 mg, 50 μmol) and KHMDS (10 mg, 50 μmol) were mixed in THF-d₈ (0.8 mL) and stirred for 30 minutes. The solution was filtered and transferred to a J-Young NMR tube for spectroscopic analysis. ³¹P{¹H} NMR (THF-d₈) δ 99.8 (d, ²J_{P,P} = 60.0 Hz, PPh₃), 64.1 (dd, ²J_{P,P} = 60.0 Hz, ³J_{P,P} = 15.0 Hz, PPh₂), 51.1 (d, ³J_{P,P} = 15.0 Hz, N=P). ¹H NMR (THF-d₈) δ 8.42 (d, ²J_{H,H} ~ 7.0 Hz and ³J_{H,H} ~ 3.0 Hz, 2H, H_{Ar}); 7.40-7.02 (m, ca. 23H, H_{Ar}), 6.59 (dd, ³J_{H,H} = 6.40 and 8.5 Hz, 1H, H₃), 6.51 (d, ³J_{H,H} ~ 8.5 Hz, 1H, H₄), 5.47 (d, ³J_{H,H} ~ 6.5 Hz, 1H, H₂), 4.26 (vt, ²J_{P,H} = 15.5 Hz and ²J_{P,H} = 16.5 Hz, 1 H, H_{6a}), 4.16 (s, H₇), 4.02 (vt, ²J_{H,H} = 15.5 Hz and ²J_{P,H} = 16.5 Hz, 1 H, H_{6b}), 2.00-1.80 (m, 4 H, H_{Cy}), 1.68-1.0 (m, 25 H, H_{Cy}), 0.91 (q, ²J_{H,H} ~ 7.5 Hz, 4 H, H_{Cy}) -12.2 (dd, ²J_{P,H} = 50.0 and 14.5 Hz, 1H, RuH). ¹³C{³¹P} NMR (THF-d₈): δ 169.3 (C^V), 140.5 (C^{IV}), 133.8, 133.3, 132.0, 130.6, 129.8, 128.3, 127.0 (C^{IV}), 125.7 (C^{IV}), 126.4, 111.3, 94.2, 69.5, 58.5, 27.2, 27.0, 26.4, 26.2.

General protocol for dehydrogenative coupling: **3^{Cy}** (148 mg, 0.012 mmol) and the primary alcohol (12 mmol) were mixed in a schlenk tube. Next, KHMDS (4.8 mg, 0.024 mmol) was added as a solid. The reaction mixture was stirred during 5 minutes and the flask was equipped with a reflux condenser. The solution was heated to reflux under nitrogen flow for 24 h. For entries 3 to 5, the reactions were performed as described above but toluene (3 mL) was added.

X-ray crystallography

Data were collected at 150 K on a Bruker Kappa APEX II diffractometer using a Mo-κ (λ=0.71069Å) X-ray source and a graphite monochromator. The crystal structures were solved using SIR 97²⁸ and refined using Shelxl-97 or Shelxl-2013.²⁹ ORTEP drawings were made using ORTEP III³⁰ for Windows or Mercury.

Conflicts of interest

The authors declare no conflict of interest.

Acknowledgements

The authors thank CNRS and Ecole polytechnique for financial support. E. Dubois is acknowledged for the synthesis of 2-(azidomethyl)-6-(hydroxymethyl)pyridine and S. Bourcier for mass spectroscopy measurements.

Notes and references

‡ Other precursors were used in order to avoid the presence of triphenylphosphine in the coordination sphere but results were disappointing. Reaction between L^{Ph} with $[RuCl_2(DMSO)]$ is slow and leads to 2 isomers differing by the coordination of the DMSO. Reaction with $[RuCl_2(nbd)]_n$ led to different products better results were obtained with $[RuCl_2(nbd)(py)_2]$.

† L^{R*} is used to label the resulting deprotonated ligand with a dearomatized pyridine ring

1. a) T. Ikariya, K. Murata and R. Noyori, *Org. Biomol. Chem.*, 2006, **4**, 393-406; b) J. I. v. d. Vlugt and J. N. H. Reek, *Angew. Chem. Int. Ed.*, 2009, **48**, 8832-8846; c) J. I. van der Vlugt, *Eur. J. Inorg. Chem.*, 2012, 363-375; d) J. R. Khusnutdinova and D. Milstein, *Angew. Chem. Int. Ed.*, 2015, **54**, 12236-12273; e) H. Li, B. Zheng and K.-W. Huang, *Coord. Chem. Rev.*, 2015, **293-294**, 116-138; f) R. H. Morris, *Acc. Chem. Res.*, 2015, **48**, 1494-1502; g) T. Zell and D. Milstein, *Acc. Chem. Res.*, 2015, **48**, 1979-1994.
2. a) T. Ohkuma, H. Ooka, S. Hashiguchi, T. Ikariya and R. Noyori, *J. Am. Chem. Soc.*, 1995, **117**, 2675-2676; b) R. Noyori and S. Hashiguchi, *Acc. Chem. Res.*, 1997, **30**, 97-102.
3. a) P. Maire, T. Büttner, F. Breher, P. L. Floch and H. Grützmacher, *Angew. Chem. Int. Ed.*, 2005, **44**, 6318-6323; b) K. Muñiz, *Angew. Chem. Int. Ed.*, 2005, **44**, 6622-6627; c) C. P. Casey and H. Guan, *J. Am. Chem. Soc.*, 2007, **129**, 5816-5817; d) T. Li, I. Bergner, F. N. Haque, M. Zimmer-De Iulius, D. Song and R. H. Morris, *Organometallics*, 2007, **26**, 5940-5949; e) M. Trincado, K. Kühlein and H. Grützmacher, *Chem. Eur. J.*, 2011, **17**, 11905-11913; f) W. Zuo, A. J. Lough, Y. F. Li and R. H. Morris, *Science*, 2013, **342**, 1080-1083; g) S. Werkmeister, K. Junge, B. Wendt, E. Alberico, H. Jiao, W. Baumann, H. Junge, F. Gallou and M. Beller, *Angew. Chem. Int. Ed.*, 2014, **53**, 8722-8726.
4. a) Y. Shvo, D. Czarkie, Y. Rahamim and D. F. Chodosh, *J. Am. Chem. Soc.*, 1986, **108**, 7400-7402; b) R. Kawahara, K. i. Fujita and R. Yamaguchi, *Angew. Chem. Int. Ed.*, 2012, **51**, 12790-12794; c) T. Yan, B. L. Feringa and K. Barta, *Nature Communications*, 2014, **5**, 5602; d) A. J. Rawlings, L. J. Diorazio and M. Wills, *Org. Lett.*, 2015, **17**, 1086-1089; e) C. M. Moore, B. Bark and N. K. Szymczak, *ACS Catal.*, 2016, **6**, 1981-1990.
5. C. Gunanathan and D. Milstein, *Chem. Rev.*, 2014, **114**, 12024-12087.
6. a) H. Salem, L. J. W. Shimon, Y. Diskin-Posner, G. Leitus, Y. Ben-David and D. Milstein, *Organometallics*, 2009, **28**, 4791-4806; b) S. Kundu, W. W. Brennessel and W. D. Jones, *Inorg. Chem.*, 2011, **50**, 9443-9453; c) G. M. Adams, F. M. Chadwick, S. D. Pike and A. S. Weller, *Dalton Trans.*, 2015, **44**, 6340-6342; d) D. W. Shaffer, I. Bhowmick, A. L. Rheingold, C. Tsay, B. N. Livesay, M. P. Shores and J. Y. Yang, *Dalton Trans.*, 2016, **45**, 17910-17917.
7. a) M. Mastalir, M. Glatz, N. Gorgas, B. Stoger, E. Pittenauer, G. Allmaier, L. F. Veiros and K. Kirchner, *Chem. Eur. J.*, 2016, **22**, 12316-12320; b) F. Bertini, M. Glatz, N. Gorgas, B. Stoger, M. Peruzzini, L. F. Veiros, K. Kirchner and L. Gonsalvi, *Chem. Sci.*, 2017, **8**, 5024-5029; c) M. Mastalir, E. Pittenauer, G. Allmaier and K. Kirchner, *J. Am. Chem. Soc.*, 2017, **139**, 8812-8815; d) M. Mastalir, E. Pittenauer, B. Stoger, G. Allmaier and K. Kirchner, *Org. Lett.*, 2017, **19**, 2178-2181.
8. a) C. Gunanathan, L. J. W. Shimon and D. Milstein, *J. Am. Chem. Soc.*, 2009, **131**, 3146-+; b) C. Gunanathan, B. Gnanaprakasam, M.

- A. Iron, L. J. W. Shimon and D. Milstein, *J. Am. Chem. Soc.*, 2010, **132**, 14763-14765.
9. a) E. Balaraman, B. Gnanaprakasam, L. J. W. Shimon and D. Milstein, *J. Am. Chem. Soc.*, 2010, **132**, 16756-16758; b) E. Balaraman, Y. Ben-David and D. Milstein, *Angew. Chem. Int. Ed.*, 2011, **50**, 11702-11705.
 10. S. Y. de Boer, T. J. Korstanje, S. R. La Rooij, R. Kox, J. N. H. Reek and J. I. van der Vlugt, *Organometallics*, 2017, **36**, 1541-1549.
 11. a) J. Zhang, G. Leitus, Y. Ben-David and D. Milstein, *Angew. Chem. Int. Ed.*, 2006, **45**, 1113-1115; b) C. Gunanathan, Y. Ben-David and D. Milstein, *Science*, 2007, **317**, 790-792; c) B. Gnanaprakasam, E. Balaraman, Y. Ben-David and D. Milstein, *Angew. Chem. Int. Ed.*, 2011, **50**, 12240-12244.
 12. a) I. M. Marín and A. Auffrant, *Eur. J. Inorg. Chem.*, 2018, 1634-1644; b) T. P. A. Cao, S. Labouille, A. Auffrant, Y. Jean, X. F. Le Goff and P. Le Floch, *Dalton Trans.*, 2011, **40**, 10029-10037; c) T. P. A. Cao, A. Buchard, X. F. Le Goff, A. Auffrant and C. K. Williams, *Inorg. Chem.*, 2012, **51**, 2157-2169; d) T. P. A. Cao, G. Nocton, L. Ricard, X. F. Le Goff and A. Auffrant, *Angew. Chem. Int. Ed.*, 2014, **53**, 1368-1372; e) I. M. Marín, T. Cheisson, R. Singh-Chauhan, C. Herrero, M. Cordier, C. Clavaguéra, G. Nocton and A. Auffrant, *Chem. Eur. J.*, 2017, **23**, 17940-17953.
 13. a) T. Cheisson, A. Auffrant and G. Nocton, *Organometallics*, 2015, **34**, 5470-5478; b) T. Cheisson and A. Auffrant, *Dalton Trans.*, 2014, **43**, 13399-13409; c) V. Cadierno, J. Diez, S. E. Garcia-Garrido, S. Garcia-Granda and J. Gimeno, *J. Chem. Soc., Dalton Trans.*, 2002, 1465-1472.
 14. T. Cheisson and A. Auffrant, *Dalton Trans.*, 2016, **45**, 2069-2078.
 15. M. W. P. Bebbington and D. Bourissou, *Coord. Chem. Rev.*, 2009, **253**, 1248-1261.
 16. a) A. Sacco, G. Vasapollo, C. F. Nobile, A. Piergiovanni, M. A. Pellinghelli and M. Lanfranchi, *J. Organomet. Chem.*, 1988, **356**, 397-409; b) M. Alvarez, N. Luga and R. Mathieu, *J. Chem. Soc., Dalton Trans.*, 1994, 2755-2760.
 17. L. Yang, D. R. Powell and R. P. Houser, *Dalton Trans.*, 2007, 955-964.
 18. X. Tan, Y. Wang, Y. Liu, F. Wang, L. Shi, K.-H. Lee, Z. Lin, H. Lv and X. Zhang, *Org. Lett.*, 2015, **17**, 454-457.
 19. A. W. Addison, T. N. Rao, J. Reedijk, J. van Rijn and G. C. Verschoor, *J. Chem. Soc., Dalton Trans.*, 1984, 1349-1356.
 20. a) C. Y. Liu, D. Y. Chen, M. C. Cheng, S. M. Peng and S. T. Liu, *Organometallics*, 1995, **14**, 1983-1991; b) C. Y. Liu, D. Y. Chen, G. H. Lee, S. M. Peng and S. T. Liu, *Organometallics*, 1996, **15**, 1055-1061.
 21. S. Chakraborty, U. Gellrich, Y. Diskin-Posner, G. Leitus, L. Avram and D. Milstein, *Angew. Chem. Int. Ed.*, 2017, **56**, 4229-4233.
 22. D. Aguilar, R. Bielsa, T. Soler and E. P. Urriolabeitia, *Organometallics*, 2011, **30**, 642-648.
 23. a) M. A. Leeson, B. K. Nicholson and M. R. Olsen, *J. Organomet. Chem.*, 1999, **579**, 243-251; b) K. T. K. Chan, L. P. Spencer, J. D. Masuda, J. S. J. McCahill, P. Wei and D. W. Stephan, *Organometallics*, 2004, **23**, 381-390; c) D. Aguilar, R. Bielsa, M. Contel, A. Lledos, R. Navarro, T. Soler and E. P. Urriolabeitia, *Organometallics*, 2008, **27**, 2929-2936; d) E. Martinez-Arripe, F. Jean-Baptiste-dit-Dominique, A. Auffrant, X. F. Le Goff, J. Thuilliez and F. Nief, *Organometallics*, 2012, **31**, 4854-4861; e) K. R. D. Johnson and P. G. Hayes, *Chem. Soc. Rev.*, 2013, **42**, 1947-1960; f) M. T. Zamora, K. R. D. Johnson, M. M. Hanninen and P. G. Hayes, *Dalton Trans.*, 2014, **43**, 10739-10750.
 24. J. Zhang, G. Leitus, Y. Ben-David and D. Milstein, *J. Am. Chem. Soc.*, 2005, **127**, 12429-12429.
 25. D. Spasyuk, S. Smith and D. G. Gusev, *Angew. Chem. Int. Ed.*, 2012, **51**, 2772-2775.
 26. R. Singler and R. D. Feltham, *Inorganic Syntheses*, 1970, **11**, 238.

27. R. A. Schunn and E. R. Wonchoba, *Inorganic Syntheses*, 1972, **13**, 131-134.
28. A. Altomare, M. C. Burla, M. Camalli, G. L. Cascarano, C. Giacovazzo, A. Guagliardi, A. G. G. Moliterni, G. Polidori and R. Spagna, *Journal of Applied Crystallography*, 1999, **32**, 115-119.
29. G. M. Sheldrick, *SHELXL-97*, Universität Göttingen, Göttingen, Germany, 1997.
30. L. J. Farrugia, *ORTEP-3 program*, (2001) Department of Chemistry, University of Glasgow.